Bioorganic & Medicinal Chemistry Letters 22 (2012) 2833–2836

Contents lists available at SciVerse ScienceDirect

Bioorganic & Medicinal Chemistry Letters

journal homepage: www.elsevier.com/locate/bmcl

Deep-red fluorescent imaging probe for bacteria

Alexander G. White [a], Brian D. Gray [b], Koon Yan Pak [b], Bradley D. Smith [a,*]

[a] Department of Chemistry and Biochemistry, 236 Nieuwland Science Hall, University of Notre Dame, Notre Dame, IN 46556, USA
[b] Molecular Targeting Technologies Incorporated, 833 Lincoln Ave., Unit 9, West Chester, PA 19380, USA

ARTICLE INFO

Article history:
Received 20 December 2011
Revised 17 February 2012
Accepted 23 February 2012
Available online 3 March 2012

Keywords:
Fluorescent molecular probe
Imaging bacterial infection
Zinc dipicolylamine
In vivo imaging
Optical imaging
FRET

ABSTRACT

A versatile deep-red fluorescent imaging probe is described that is comprised of a bis(zinc(II)-dipicolylamine) targeting unit covalently attached to a pentamethine carbocyanine fluorophore with Cy5-like spectroscopic properties. A titration assay based on fluorescence resonance energy transfer is used to prove that the probe selectively associates with anionic vesicle membranes whose composition mimics bacterial cell membranes. Whole-body optical imaging experiments show that the probe associates with the surfaces of both Gram-positive and Gram-negative bacteria cells, and it can target the site of bacterial infection in a living mouse. In vivo accumulation at the infection site and subsequent clearance occurs more quickly than a structurally related near-infrared bis(zinc(II)-dipicolylamine) probe. The fact that the same deep-red probe molecule can be used for spectroscopic assays, cell microscopy, and in vivo imaging studies, is an important and attractive technical feature.

Over the last five years we have developed a series of fluorescent bis(zinc(II)-dipicolylamine) (bis(Zn-DPA)) imaging probes that target anionic membranes and these molecular probes have proven useful for optical imaging of two major classes of cells: dead and dying mammalian cells and bacterial cells.[1] Initially, we synthesized blue and green emitting bis(Zn-DPA) probes that were suitable for bacterial cell studies using flow cytometry and fluorescence microscopy.[2] We have also developed a near-infrared version that is very effective for in vivo imaging studies of infection models in rodents.[3] Imaging probes that incorporate a deep-red fluorophore with excitation/emission wavelengths that match the common Cy5 filter set (approximately 645/665 nm) in microscopes, microarrays, and flow cytometers are particularly useful.[4] This wavelength region is still visible to the eye of a microscope operator which facilitates microscopic studies, yet it is sufficiently red to allow effective in vivo imaging in living animals.[4c,d] Performance limitations, due to undesired absorption and autofluorescence by endogenous biomolecules and scattering of the light by animal skin and tissue, are attenuated at longer wavelengths.[5] Previously, we have reported deep-red bis(Zn-DPA) probes with structurally unusual squaraine rotaxane fluorophores,[6] but the need remains for additional deep-red bis(Zn-DPA) probes that are relatively cheap to produce. A low production cost is extremely important for many imaging applications that require large amounts of probe material such as high throughput cell screening assays or temporal studies of large cohorts of animal models.[7] Here, we describe the new and versatile deep-red probe, **1**, that is comprised of a bis(Zn-DPA) targeting unit covalently attached to a pentamethine carbocyanine fluorophore with Cy5-like spectroscopic properties (Scheme 1). We demonstrate how this probe can be used in a spectrometric Fluorescence Resonance Energy Transfer (FRET) assay that measures probe association with model vesicle membranes of any phospholipid composition. We also show how probe **1** can be used to stain bacteria cells and optically image sites of bacterial infection in a living mouse.

The straightforward synthesis of probe **1** using readily available building blocks is described in the Supplementary data. In short, the bis(Zn-DPA) unit is coupled to the carbocyanine fluorophore by forming an amide-bond.[8] Probe **1** is highly water soluble and exhibits attractive photophysical properties in aqueous solution (λ_{abs} = 643 nm, ε = 42,800 M^{-1} cm^{-1}, λ_{em} = 658 nm, ϕ_f = 0.13). Based on previous experience, we expected that the bis(Zn-DPA) unit would promote association with membrane surfaces that are rich in anionic phospholipids. One example is the bacterial membrane. The cellular envelope of Gram-positive bacteria is rich in phosphatidylglycerol and other phosphorylated amphiphiles, and the outer membrane of Gram-negative bacteria is known to contain a large fraction of lipopolysaccharides that have anionic Lipid A as the core structure (Scheme 1).[2] Before starting the bacterial studies we wanted to measure the association of probe **1** with model vesicles that mimic bacterial cell membranes. It is a technical challenge to quantitatively measure the binding of small molecules to bilayer membranes.[9] We were attracted to the Cy5-like, carbocyanine fluorophore in probe **1** because it can accept energy from a donor Cy3-like chromophore via a FRET pathway.[10] Thus,

* Corresponding author. Tel.: +1 574 631 8632; fax: +1 574 631 6652.
E-mail address: smith.115@nd.edu (B.D. Smith).

0960-894X/$ - see front matter © 2012 Elsevier Ltd. All rights reserved.
doi:10.1016/j.bmcl.2012.02.078

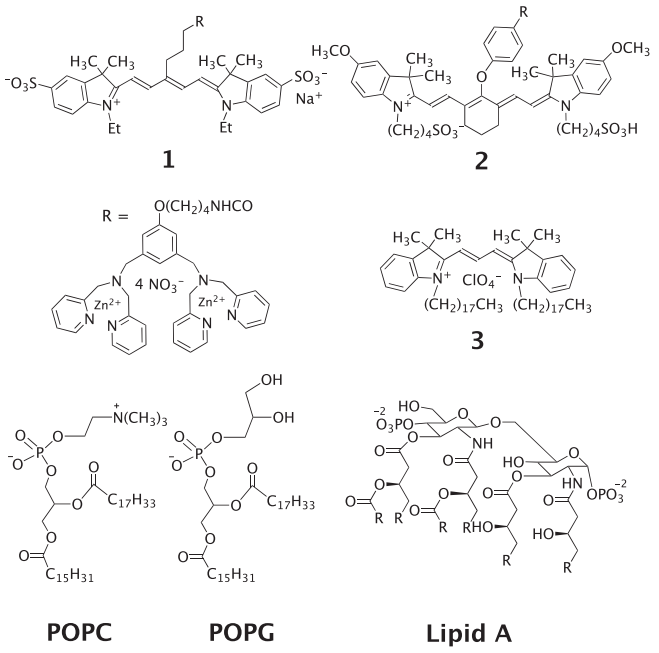

Scheme 1. Chemical structures of the fluorescent probes and phospholipids used in this study.

we constructed a FRET based titration assay for membrane binding (Fig. 1A). The lipophilic dye **3** (also known as $DiIC_{18}$) was incorporated into the membrane of vesicles and then probe **1** was added in incremental amounts. Association of **1** to membranes leads to strong energy transfer, which is observed as a loss in the donor emission band at 570 nm and an increase in the acceptor emission band at 665 nm. The spectral data in Figure 1B–D is plotted in Figure 1E as a set of titration isotherms. The plots show that probe **1** has very weak affinity for zwitterionic membranes composed of 1-palmitoyl-2-oleoyl-*sn*-glycero-3-phosphocholine (POPC), and stronger affinity for membranes that are enriched in Lipid A (mimic of Gram-negative membrane) or1-palmitoyl-2-oleoyl-*sn*-glycero-3-phosphoglycerol, (POPG, mimic of Gram-positive bacteria). These titration curves fitted well to a binding model of the probe forming a 1:1 complex with the anionic phospholipid that is exposed on the outer surface of the vesicle. The association constant for membranes that are rich in Lipid A ($1.2 \times 10^5\ M^{-1}$) is higher than for membranes that are rich in POPG ($1.3 \times 10^4\ M^{-1}$). This is structurally reasonable since the polar head group of the Lipid A structure contains two dianionic phosphate monoesters groups (Scheme 1) that have an inherently higher affinity for the cationic bis(Zn-DPA) unit in probe **1**. The titration curves also show a lower extent of FRET for **1** binding to Lipid A-rich membranes, reflecting the five times lower number of membrane binding sites for the same amount of FRET donor dye **3**. From an operational

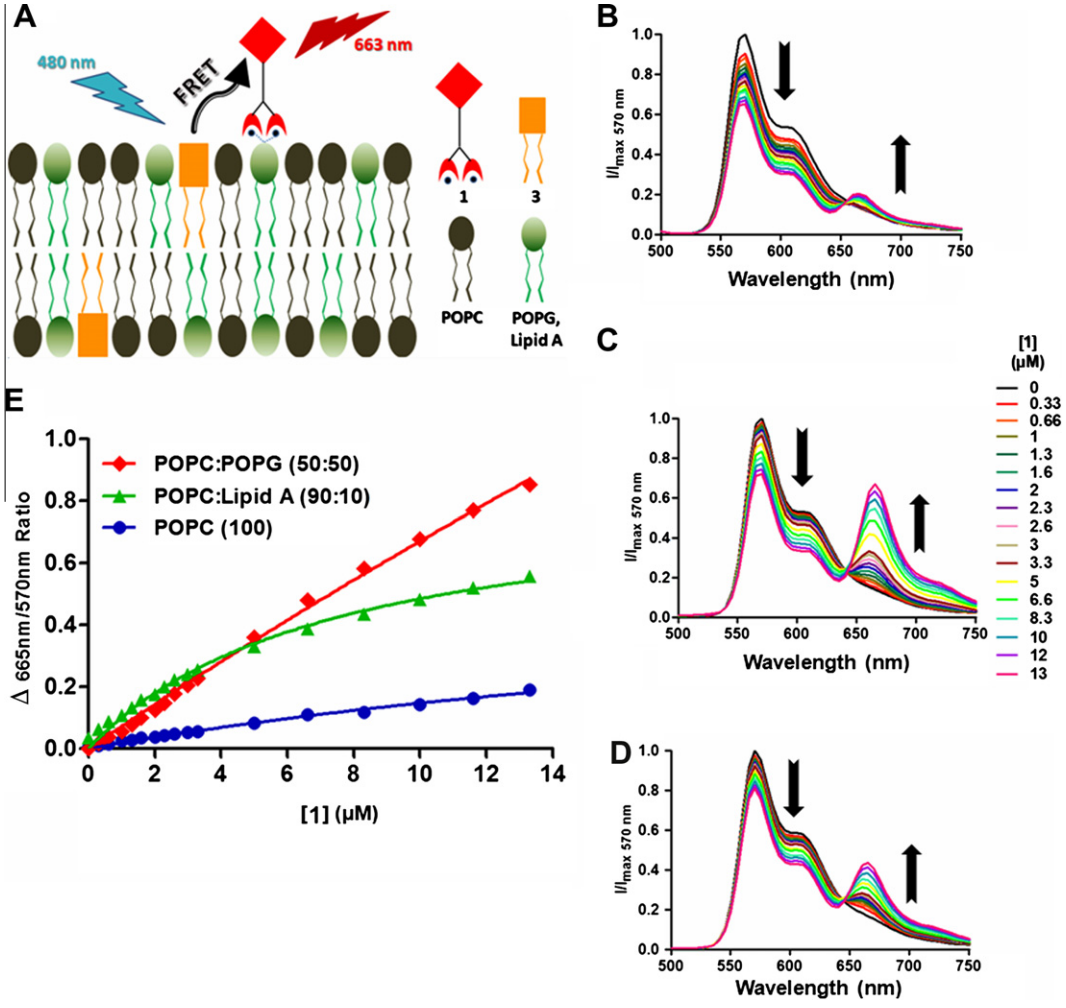

Figure 1. Association of fluorescent energy acceptor **1** to the surface of vesicles containing 1 mol % of the energy donor **3** induces FRET. (A) Schematic of the FRET process. (B, C, D) Normalized spectra of FRET induced by incremental addition of **1** to vesicles containing **3** and composed of only POPC, POPC/POPG (50:50), or POPC/lipid A (90:10), respectively. (E) Plots of the spectral data showing changes in the ratio of acceptor/donor fluorescence intensities due to association-induced FRET.

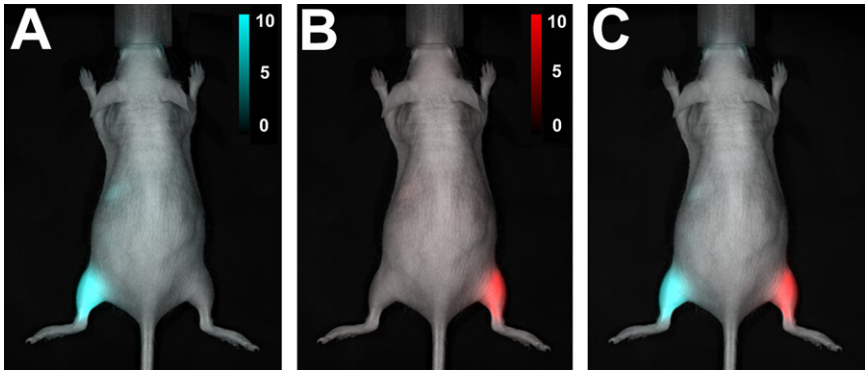

Figure 2. Optical imaging of anesthetized hairless mouse with separate rear leg injections of *S. aureus* Xen31 (~10^8 cells) prelabeled with 10 nmol of either **1** (A, cyan color showing deep-red signal via the Cy5.5 filter set) or **2** (B, red color showing infrared signal via the ICG filter set). Panel C shows an overlaid image of the spectrally unmixed emission signals from the two populations of *S. aureus* Xen31 labeled with **1** or **2**. Intensity scale for each image is in arbitrary units. $N = 3$.

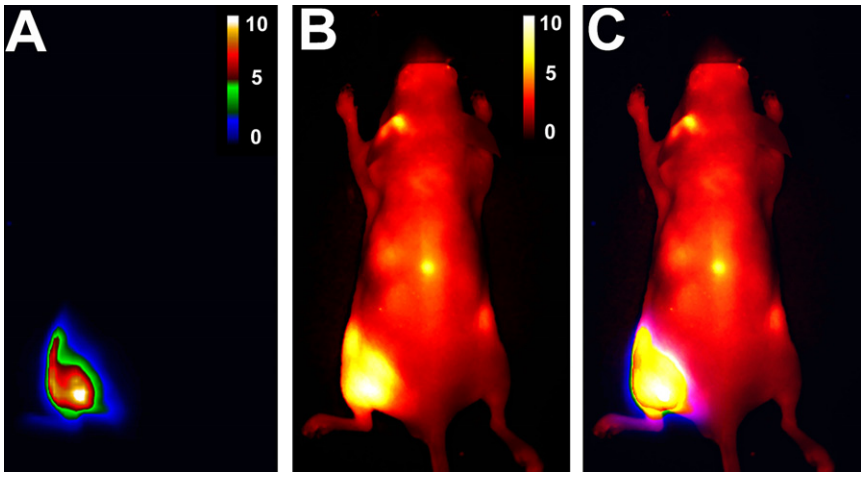

Figure 3. Optical imaging of anesthetized hairless mouse with a rear leg injection of bioluminescent *S. typhimurium* AM3 (~10^8 cells) and treated 3 h later with 10 nmol of **1** via the tail vein. (A) Bioluminescent signal from bacteria, (B) fluorescent signal from **1**, (C) overlay of panels A and B. Images were acquired 3 h after probe dosage. Intensity scale for each image is in arbitrary units. $N = 3$.

perspective we find that this FRET-based vesicle binding assay is technically straightforward to conduct and highly reproducible. The fact that it can be used to measure association of **1** with vesicles of any composition makes it highly versatile.

The outer membrane surface of healthy animal cells is composed primarily of zwitterionic phospholipids, and we have previously shown that bis(Zn-DPA) probes can selectively target sites of bacterial infection in living animals.[2,3] The vesicle titration data in Figure 1 suggested that probe **1** should also exhibit selective and universal affinity for the cell envelope of virtually all genera of bacteria.[2,3,6] This hypothesis was confirmed first by conducting pelleting experiments that treated representative strains of Gram-positive and Gram-negative bacteria (*Staphylococcus aureus*, *Escherichia coli, Salmonella typhimurium*) with probe **1** and showing in each case that the bacterial pellet, produced after centrifugation and washing, exhibited intense deep-red fluorescence. A subsequent animal imaging experiment demonstrated that the deep-red fluorescence could be observed through skin and tissue. Specifically, two separate populations of Gram-positive *Staphylococcus aureus* Xen31 were mixed with either deep-red probe **1** or the known near-infrared probe **2** (excitation/emission wavelengths of 794/810 nm)[3] and each cell/probe mixture was converted into a pellet by centrifugation. The two pellets were washed and then injected into the opposite rear legs of an anesthetized mouse, and a whole-body optical image of the mouse was recorded using an in vivo animal imaging station. The images in Figure 2 show that both probes have good affinity for the *S. aureus* and that the deep-red fluorescence signal for **1** could be observed separately from the near-infrared signal of **2**.

Next, two sets of animal imaging experiments demonstrated the effectiveness of probe **1** to selectively target a bacterial infection within a living mouse. In each case, a bolus of ~10^8 bacterial cells was injected into the rear leg of an anesthetized mouse and then, 3 h later, a dose of probe **1** (10 nmol) was injected intravenously via the tail vein. The whole-body images in Figure 3 were acquired at 3 h after the probe injection. In this case, the infection was a bioluminescent strain of *Salmonella typhimurium* AM3, a Gram-negative bacteria. Shown in Figure 3A is the bioluminescent emission from the *S. typhimurium*, and in Figure 3B is a deep-red fluorescence image. The overlaid image in Figure 3C confirms that probe **1** is highly colocalized at the same anatomical site as the bioluminescent bacteria.

The images in Figure 4 summarize an analogous experiment that used probe **1** to target an infection of Gram-positive *S. aureus* Xen31. The montage shows the accumulation of probe **1** and its subsequent clearance from the animal. A region-of-interest analysis of these in vivo images indicated that the maximum target to background ratio of 4.2 was achieved after 6 h, and that there was very little fluorescent signal remaining at the site of bacterial infection after 24 h. This latter fact was confirmed with an ex vivo

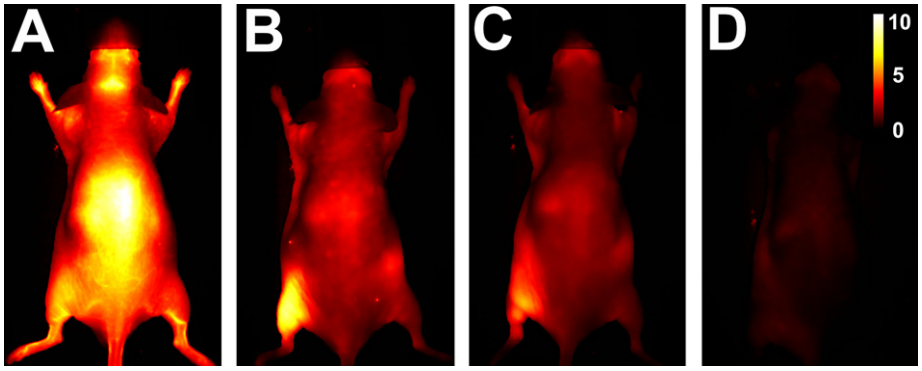

Figure 4. Fluorescence imaging montage of anesthetized hairless mouse containing a rear leg injection of *S. aureus* Xen31 ($\sim 10^8$ cells) and treated 3 h later with 10 nmol of **1** via the tail vein. Mouse was imaged at (A) 0 h, (B) 3 h, (C) 6 h, and (D) 24 h after probe dosage. Intensity scale (arbitrary units) applies to all images. $N = 4$.

biodistribution analysis of the excised tissues after animal sacrifice at 24 h (see Fig. S4). A comparison of the in vivo imaging data in Figure 4 with literature shows that probe **1** (10 nmol) can be employed at about a fourfold lower dosage than probe **2** for the same T/NT ratio.[3] Furthermore, probe **1** washes out much faster from the infection site than probe **2**. This suggests that probe **1** may be better suited for longitudinal imaging studies that must repeatedly image the same infected animal over time.[11] Fluorescent probes like **1** and **2** with a single bis(Zn-DPA) targeting unit can detect a mouse leg infection containing $\sim 10^7$ or more bacterial cells, but this visualization threshold can be lowered by using higher affinity bacterial probes whose chemical structures containing multiple bis(Zn-DPA) units.[6] While the tissue penetration of near-infrared light associated with **2** is slightly greater than the red light of **1**, neither probe is expected to be very useful for fluorescent planar imaging of deep tissue infection sites in larger animals. However, continued advances in fluorescence tomography may ameliorate this technical limitation.[7g]

In summary, we find that deep-red bis(Zn-DPA) probe **1** exhibits several useful photophysical and supramolecular properties that make it a very attractive and versatile targeted probe for fluorescence imaging studies of membranes that are rich in anionic phospholipids. The probe can be employed in a technically straightforward FRET-based assay that measures affinity for model vesicle membranes of any composition. The bis(Zn-DPA) unit in probe **1** selectively targets the abundant phosphorylated amphiphiles within the cell envelope of Gram-positive and Gram-negative bacteria.[2,3,6] Thus, probe **1** is expected to be a universal fluorescent imaging probe for any bacterial infection in a living mouse. The fact that the same probe molecule can be used for spectroscopic assays, cell microscopy, and in vivo imaging studies, is an important technical feature that simplifies the experimental design and reduces experimental uncertainty since there is no change in probe molecular structure.

Acknowledgments

This work was supported by the NIH (GM059078 to B.D.S.) and the Notre Dame Integrated Imaging Facility. All animal care and imaging protocols were approved by the Notre Dame Institutional Animal Care and Use Committee. We are grateful to members of the Freimann Life Sciences Center for professional animal care.

Supplementary data

Supplementary data (probe synthesis, experimental methods, imaging analyses) associated with this article can be found, in the online version, at doi:10.1016/j.bmcl.2012.02.078.

References and notes

1. (a) O'Neil, E. J.; Smith, B. D. *Coord. Chem. Rev.* **2006**, *250*, 3068–3080; (b) Drewry, J. A.; Gunning, P. T. *Coord. Chem. Rev.* **2011**, *255*, 459.
2. Leevy, W. M.; Johnson, J. R.; Lakshmi, C.; Morris, J.; Marquez, M.; Smith, B. D. *Chem. Commun.* **2006**, *15*, 1595.
3. (a) Leevy, W. M.; Gammon, S. T.; Jiang, H.; Johnson, J. R.; Maxwell, D. J.; Marquez, M.; Piwnica-Worms, D.; Smith, B. D. *J. Am. Chem. Soc.* **2006**, *128*, 16476; (b) Leevy, W. M.; Gammon, S. T.; Johnson, J. R.; Lampkins, A. J.; Jiang, H.; Marquez, M.; Piwnica-Worms, D.; Suckow, M. A.; Smith, B. D. *Bioconjugate Chem.* **2008**, *19*, 686.
4. (a) Terai, T.; Nagano, T. *Curr. Opin. Chem. Biol.* **2008**, *12*, 515; (b) Trinquet, E.; Mathis, G. *Mol. Biosyst.* **2006**, *2*, 380; (c) Enniga, J.; Sansonetti, P.; Tournebize, R. *Trends Microbiol.* **2007**, *15*, 483; (d) Hoppe, A. D.; Seveau, S.; Swanson, J. A. *Cell. Microbiol.* **2009**, *11*, 540.
5. Kobayashi, H.; Ogawa, M.; Alford, R.; Choyke, P. L.; Urano, Y. *Chem. Rev.* **2010**, *110*, 2620.
6. (a) Johnson, J. R.; Fu, N.; Arunkumar, E.; Leevy, W. M.; Gammon, S. T.; Piwnica-Worms, D.; Smith, B. D. *Angew. Chem. Int. Ed.* **2007**, *46*, 5528; (b) White, A. G.; Fu, N.; Leevy, W. M.; Lee, J. J.; Blasco, M. A.; Smith, B. D. *Bioconjuate. Chem.* **2010**, *21*, 1297.
7. (a) Leevy, W. M.; Serazin, N.; Smith, B. D. *Drug Discovery Today* **2007**, *4*, 91; (b) Zhao, X. J.; Hilliard, L. R.; Mechery, S. J.; Wang, Y. P.; Bagwe, R. P.; Jin, S. G.; Tan, W. H. A. *Proc. Natl. Acad. Sci. U.S.A.* **2004**, *101*, 15027; (c) Qu, L. W.; Luo, P. G.; Taylor, S.; Lin, Y.; Huang, W. J.; Anyadike, N.; Tzeng, T. R. J.; Stutzenberger, F.; Latour, R. A.; Sun, Y. P. *J. Nanosci. Nanotechnol.* **2005**, *5*, 319; (d) Zhu, C.; Yang, Q.; Liu, L.; Wang, S. *Angew. Chem. Int. Ed.* **2011**, *50*, 9607; (e) Inglese, J.; Johnson, R. L.; Simeonov, A.; Xia, M.; Zhang, W.; Austin, C. P.; Auld, D. S. *Nat. Chem. Biol.* **2007**, *3*, 466; (f) Ning, X.; Lee, S.; Wang, Z.; Kim, D.; Stubblefield, B.; Gilbert, E.; Murthy, N. *Nat. Mater.* **2011**, *10*, 602; (g) Signore, A.; Mather, S. J.; Piaggio, G.; Malviya, G.; Dierckx, R. A. *Chem. Rev.* **2010**, *110*, 3112; (h) Kong, Y.; Yao, H.; Ren, H.; Subbian, S.; Cirillo, S. L. G.; Saccettini, J. C.; Rao, J.; Cirillo, J. D. *Proc. Natl. Acad. Sci. U.S.A.* **2010**, *107*, 12239; (i) Melican, K.; Richter-Dahlfors, A. *Curr. Opin. Microbiol.* **2009**, *12*, 31.
8. (a) Shao, F.; Yuan, H.; Josephson, L.; Weissleder, R.; Hilderbrand, S. A. *Dyes Pigments* **2011**, *90*, 119; (b) Joeri, K. J.; Buckle, T.; Yuan, H.; van den Berg, N. S.; Oishi, S.; Fujii, N.; Josephson, L.; van Leeuwen, F. W. B. *Bioconjugate Chem.* **2011**, *22*, 859.
9. (a) Hofmann, A.; Huber, R. *Methods Enzymol.* **2003**, *372*, 186–216; (b) Surman, A. J.; Kenny, G. D.; Kumar, D. K.; Bell, J. D.; Casey, D. R.; Vilar, R. *Chem. Commun.* **2011**, *47*, 10245.
10. (a) Massey, M.; Algar, W. R.; Krull, U. J. *Anal. Chim.* **2006**, *568*, 181–189; (b) You, M.; Li, E.; Wimley, W. C.; Hristova, K. *Anal. Biochem.* **2005**, *340*, 154.
11. While a complete toxicity study has not yet been conducted, it is worth noting that the mice easily tolerate the presence of probe **1** (10 nmol) for at least 24 h, as judged by their continued grooming and nesting activities.